

## Enhanced oxidative desulfurization over silica-gel-immobilized heteropoly acids

A.G. Ali-Zada<sup>1\*</sup>, I.G. Tarkhanova<sup>2</sup>, V.M. Zelikman<sup>2</sup>

<sup>1</sup>Azerbaijan State Oil and Industry University, 20 Azadliq, Baku AZ1010, Azerbaijan

<sup>2</sup>Department of Chemistry, Lomonosov Moscow State University, Leninskie Gory, 1 Moscow 119991, Russia

email: [ali.alizada.g@asoiu.edu.az](mailto:ali.alizada.g@asoiu.edu.az)

### Abstract

The development of efficient oxidative desulfurization catalysts is essential for producing clean fuels under mild conditions. In this work, phosphomolybdic (PMo) and phosphotungstic (PW) heteropoly acids were immobilized onto silica gel supports by ion-exchange methods and compared with analogous Silochrom-supported systems. The catalysts were characterized using SALDI mass spectrometry, SEM, and EDX spectroscopy to assess the structural integrity of the heteropoly anions and the uniformity of their distribution on the support surface. Catalytic activity was evaluated in the oxidation of model sulfur compounds — thiophene, dibenzothiophene (DBT), and methyl phenyl sulfide — as well as in a straight-run diesel fraction (1080 ppm S) using hydrogen peroxide as the oxidant. Both catalysts achieved maximum conversion of model fuel sulfur compounds (MFSCs) within the first hour of reaction, with thiophene conversions of 69–70% and DBT conversions of 76–78%. Optimal results were obtained at an H<sub>2</sub>O<sub>2</sub>:S ratio of 20:1 and 60°C, and sequential oxidant addition further improved thiophene conversion. Importantly, silica gel-supported catalysts displayed greater stability over five consecutive cycles compared to Silochrom analogues, with consistent MFSC conversions of 100%.

**Keywords:** oxidative desulfurization, polyoxometalates, phosphomolybdic acid, silica gel, SALDI mass spectrometry.

PACS numbers: 88.20.tf, 82.33.-z, 82.65.+r

<i>Received:</i> 13 October 2025	<i>Revised:</i> 26 April 2026	<i>Accepted:</i> 4 May 2026	<i>Published:</i> 31 May 2026
-------------------------------------	----------------------------------	--------------------------------	----------------------------------

### 1. Introduction

The growing demand for clean fuels with ultra-low sulfur content has placed oxidative desulfurization (ODS) at the forefront of modern catalysis research [1,2]. Traditional hydrodesulfurization (HDS) processes, though effective for the removal of a wide range of sulfur compounds, require high temperatures and pressures, as well as significant hydrogen consumption [3,4]. Moreover, HDS often shows limited efficiency in removing refractory sulfur-containing species such as dibenzothiophene (DBT) and its alkylated derivatives, which are particularly resistant due to steric hindrance and electron delocalization within the aromatic system. Therefore, the development of alternative catalytic approaches that can operate under milder conditions, with enhanced selectivity and efficiency toward these challenging substrates, remains an urgent issue [5,6].

Polyoxometalates (POMs) have attracted considerable attention as promising candidates for ODS due to their unique redox properties, structural diversity, and the ability to act as

electron reservoirs. Phosphomolybdic (PMo) and phosphotungstic (PW) heteropoly acids, in particular, have been widely studied because of their strong Brønsted acidity and high oxidative potential [7,8]. However, their homogeneous application poses challenges such as difficult catalyst recovery, limited recyclability, and possible leaching under reaction conditions. Immobilization of POMs onto solid supports has been extensively explored as a strategy to overcome these drawbacks, enhancing both the stability and reusability of the catalysts while maintaining their intrinsic activity [9].

Silica-based materials, owing to their high surface area, tunable porosity, and chemical inertness, are particularly promising supports for POM immobilization, and the nature of the support has been shown to critically influence catalyst morphology, active-site distribution, and overall catalytic performance. In particular, catalysts based on Silochrom—a porous silica material—have been successfully employed for POM deposition [10]. Nevertheless, challenges remain in ensuring uniform distribution of the active component and preventing partial decomposition of the heteropoly anion during synthesis. A systematic comparison of different silica carriers is therefore essential to evaluate their effects on the structure, stability, and catalytic performance of immobilized POM systems [11,12].

Among surface-sensitive techniques, SALDI mass spectrometry enables molecular-level analysis of heteropoly anion integrity on catalyst surfaces, while SEM and EDX provide complementary information on particle morphology and elemental distribution [13–15].

Despite the growing interest in POM-based ODS catalysts and the variety of solid supports explored for their immobilization, a systematic comparison of different silica carriers — specifically silica gel versus Silochrom — remains lacking. In particular, the influence of the support nature on the structural integrity of the heteropoly anions during immobilization, the uniformity of active-phase distribution across the surface, and the long-term catalytic stability and recyclability of the resulting systems has not been adequately addressed. Furthermore, the application of advanced surface-sensitive characterization techniques such as SALDI mass spectrometry to probe molecular-level changes in immobilized POMs on different supports has received limited attention in the literature [16].

In this work, phosphomolybdic and phosphotungstic acids were immobilized onto silica gel supports via ion-exchange methods, and their physicochemical properties were compared with analogous catalysts supported on Silochrom. Comprehensive characterization was carried out using SALDI mass spectrometry, SEM, and EDX, providing information on the stability of heteropoly anions, particle size distribution, and surface homogeneity. The catalytic performance of these systems was evaluated in the oxidative desulfurization of model sulfur compounds, including thiophene, DBT, and methyl phenyl sulfide, as well as in the treatment of a straight-run diesel fraction. Special attention was given to the effects of catalyst loading, oxidant volume, sequential oxidant addition, and reaction temperature on substrate conversion.

This study thus provides new insights into the relationship between catalyst structure, support nature, and catalytic behavior in oxidative desulfurization. By integrating advanced surface characterization with catalytic testing, it contributes to the rational design of robust and efficient POM-based heterogeneous catalysts for clean fuel production [17-18].

## 2. Experiments

### 2.1. Surface-activated laser desorption/ionization (SALDI) mass spectrometry

Surface-activated laser desorption/ionization (SALDI) mass spectrometry was employed to investigate the molecular composition of the compounds and their spatial distribution across the catalyst surface. The analysis was conducted under the supervision of Prof. A.K. Buryak at the Chromatography Laboratory of the A.N. Frumkin Institute of Physical Chemistry and Electrochemistry, Russian Academy of Sciences. SALDI mass spectra of the studied samples were obtained in RP Pep Mix mode using a Bruker Ultraflex mass spectrometer equipped with a nitrogen laser ( $\lambda = 337$  nm, pulse energy = 110  $\mu$ J). The mass analyzer operated in a time-of-

flight configuration. Spectra were recorded in both positive- and negative-ion modes. Cluster ion identification based on isotopic distribution was performed using the IsoPro simulation software [19].

Laser operating parameters:

- Wavelength: 337 nm
- Pulse width (FWHM): 3 ns
- Pulse energy: 1–100  $\mu$ J
- Pulse power: 45 W
- Repetition rate: 20 Hz
- Beam divergence: 3 mrad

### **2.2. Scanning electron microscopy (SEM)**

The surface morphology of the catalyst samples was characterized using a JEOL JSM-6000 NeoScope scanning electron microscope equipped with an EX-230 energy-dispersive X-ray (EDX) analyzer. Micrographs were acquired under high-vacuum conditions at an accelerating voltage of 15 kV. Secondary electron imaging (SEI) mode was employed for surface visualization. The study was carried out under the supervision of S.V. Dvoryak, engineer at the Department of Physical Chemistry.

### **2.3. Catalytic testing methodology**

The catalytic activity of immobilized IL was measured using model mixtures of thiophene, dibenzothiophene, and methyl phenyl sulfide (thioanisole), as well as straight-run diesel fraction provided by OAO “Varyeganneft,” with an initial sulfur content of 1080 ppm [20].

### **2.4. Oxidation of thiophene, dibenzothiophene, and thioanisole with hydrogen peroxide in isooctane**

In a thermostatted reactor, 10 mL of the model mixture (1 wt.%, solution in isooctane), the catalyst (0.02–0.8 g), and the oxidizer – 50% hydrogen peroxide (0.2–0.8 mL) were placed. The contents of the reactor were stirred under heating (40–70 °C), with samples periodically taken from the liquid phase for analysis [21].

### **2.5. Oxidative desulfurization of straight-run diesel fraction**

In a jacketed reactor equipped with a magnetic stirrer, 20 mL of fuel (total sulfur – 1080 ppm), 0.02–0.08 g of catalyst, and 0.4 mL of oxidizer (50% hydrogen peroxide) were added. The mixture was stirred for 3 h at a temperature of 60 °C. Afterwards, to remove oil oxidation products and catalyst residues, the mixture was washed in the following sequence: with water, twice with a 95% solution of dimethylformamide in water, and again with water (in all cases, the volume ratio was 1:1). Then the mixture was placed back into the reactor, and after adding 0.4 mL of H<sub>2</sub>O<sub>2</sub>, it was stirred for another 3 h. At the end of the reaction, the mixture was washed again in the above-described sequence [22].

### **2.6. Methods of analysis of reaction solutions - gas-liquid chromatography**

Quantitative analysis of the organic phase in the reaction mixture was carried out by gas-liquid chromatography on a “Crystal 4000” instrument with a Zebron ZB-1 capillary column, 30 m in length. The composition of the liquid phase was 100% dimethylpolysiloxane; flame ionization detector – FID. The content of sulfur-containing compounds was determined in the linear programming mode at temperatures of 90–260 °C using the internal standard method. Dodecane was introduced as the standard [23].

### **2.7. Synthesis of catalytic systems based on oxometallates**

Deposition of phosphomolybdic (PMoA) and phosphotungstic (PTA) heteropoly acids (HPA) was carried out via an ion-exchange reaction. For this purpose, 0.5 g of PMoA (or 0.6 g

of PTA) was dissolved in 15 mL of ethanol, after which a weighed portion of the support, previously modified as described above, was introduced and stirred for 24 h. The liquid phase was decanted, and the sample was washed twice with ethanol and treated according to the procedure described in [24]. At this stage, volatile products were removed from the sample placed in an ampoule under vacuum at 85–90 °C [25].

By this method, the catalysts PMo-Perlkat and PW-Perlkat, PMo-Perlkatn and PW-Perlkatn, as well as PMo-Silochrom and PW-Silochrom, were obtained (figure 1). For the preparation of PMo-Perlkatn and PW-Perlkatn catalysts, the amount of heteropoly acid used in the synthesis was reduced by half.

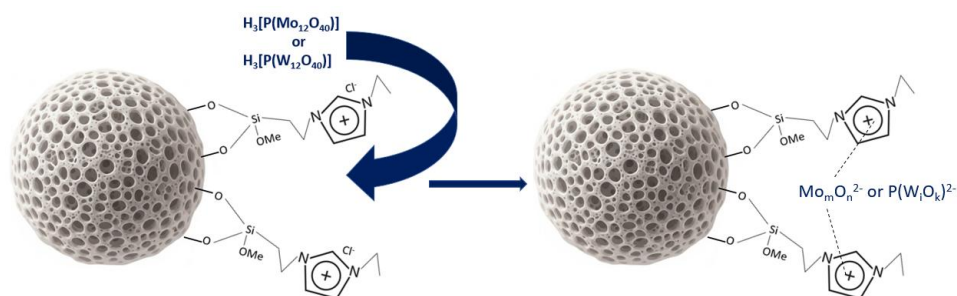


**Figure 1.** Scheme of deposition of heteropoly acids on modified supports.  $m = 2-5$ ;  $n = 7-13$ ;  $i = 2-7$ ;  $k = 4-20$

### 3. Results and discussion

#### 3.1. SALDI and SEM analysis

For the PMo–silica gel and PW–silica gel catalysts, partial destruction of the heteropoly acids (HPAs) occurs during synthesis, which is more pronounced in the tungsten-containing system. In the SALDI mass spectrum of the PMo–silica gel catalyst (figure 2), along with polymolybdate species  $\text{Mo}_2\text{O}_6$ ,  $\text{Mo}_3\text{O}_9$ ,  $\text{Mo}_4\text{O}_{12}$ ,  $\text{Mo}_5\text{O}_{15}$ , and  $\text{Mo}_6\text{O}_{18}$ , fragments of heteropolyanions are also present:  $\text{PMo}_5\text{O}_{12}$ ,  $\text{PMo}_4\text{O}_{15}$ ,  $\text{PMo}_{14}\text{O}_{42}$ , and  $\text{PMo}_{15}\text{O}_{45}$ .

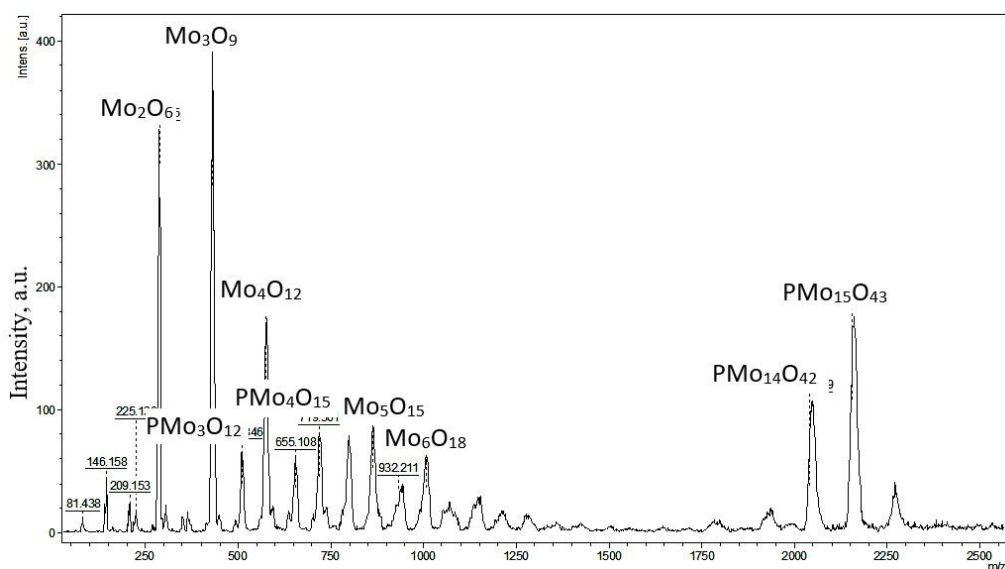


**Figure 2.** SALDI mass spectrum of the PMo–silica gel sample

As can be seen from the mass spectrum (figure 3) for the PW–silica gel catalyst, the destruction occurs to a much greater extent, as evidenced by the presence of only a single HPA fragment —  $\text{PW}_5\text{O}_{13}$  — along with poly-tungstate species  $\text{WO}_3$ ,  $\text{W}_2\text{O}_6$ ,  $\text{W}_3\text{O}_9$ , and  $\text{W}_4\text{O}_{12}$ .

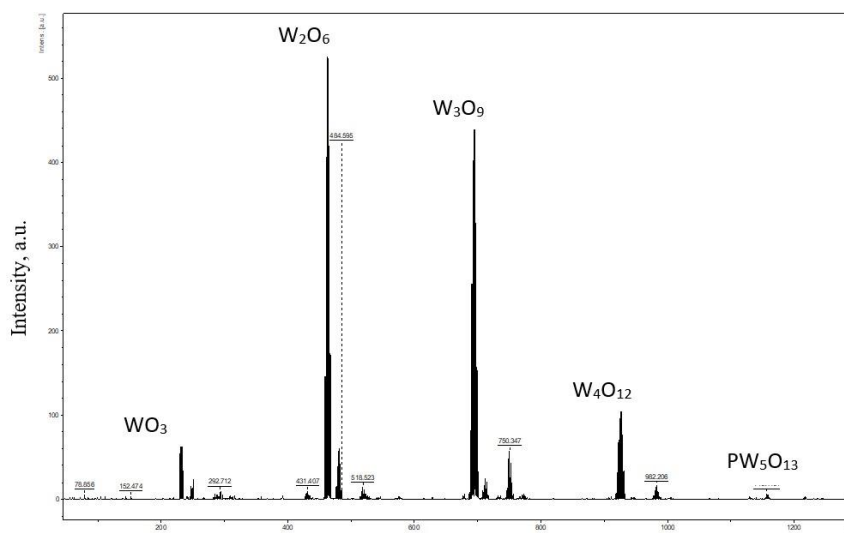


**Figure 3.** SALDI mass spectrum of the PW–silica gel sample

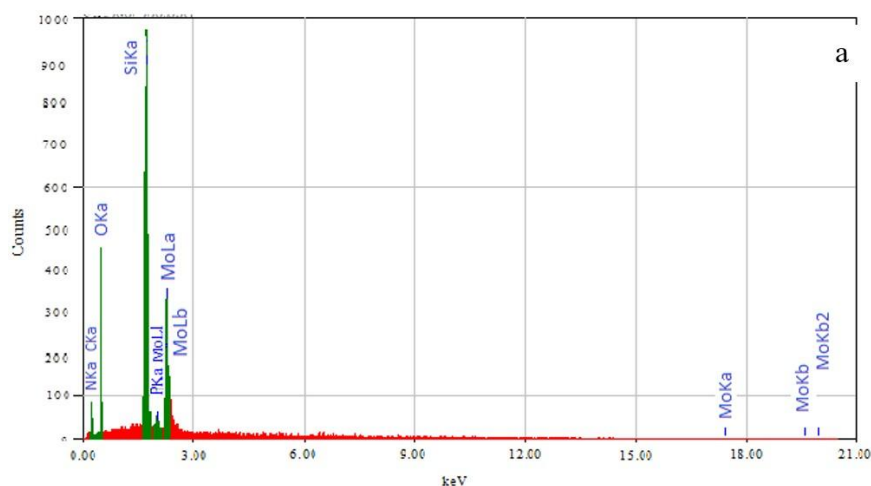


**Figure 4.** SEM micrographs and EDX spectra of the PMo–silica gel

Analysis of the SEM micrographs and EDX spectra for the PMo–silica gel (figure 4) and PW–silica gel (figure 5) samples reveal the presence of C, O, Si, P, Mo, and W, which overall corresponds to the structures proposed in figures 2 and 3.

As evident from the SEM images, the catalysts consist of larger particles compared to the analogous catalysts supported on Silochrom. The localization of phosphorus coincides with that of the metal, while the elemental distribution on the surface is more uniform than in the case of Silochrom.

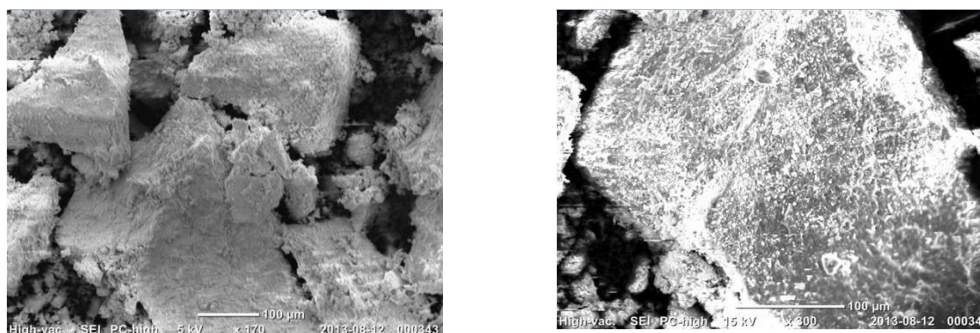


**Figure 5.** SEM–EDX spectrum (a), surface images of the sample (b)

In the PW–silica gel catalyst (figure 5), the distribution of phosphorus coincides with that of the metal. Analysis of the phosphorus and tungsten mapping data indicates that the elements are uniformly distributed over the catalyst surface.

It should be noted that the deposited heteropoly acid phase is expected to be predominantly amorphous. This inference is supported by several observations: the SALDI mass spectra indicate partial fragmentation of the Keggin-type anions during immobilization, which is inconsistent with the preservation of long-range crystalline order; the synthesis conditions — ion-exchange deposition from ethanol solution followed by vacuum drying at 85–90 °C — typically yield amorphous or poorly crystalline deposits; and the SEM images do not reveal faceted or geometrically regular features characteristic of crystalline particles.

### 2.1. Catalytic activity of polyoxometalates immobilized on silica gel

Figures 6 and 7 present the typical time–conversion profiles for substrates over the polyoxometalate catalysts supported on silica gel. Similar to the case of catalysts on a Silochrom support, the initial oxidation rate of DBT was found to be higher than that of thiophene.

For both systems, the oxidation of model fuel sulfur compounds (MFSCs) reaches maximum conversion within the first hour of the reaction. The maximum conversions of thiophene and DBT obtained with the silica gel–supported catalysts are higher than those observed for the analogous Silochrom-supported systems. In the case of the PMo–silica gel catalyst, the conversion in thiophene oxidation was 69%, while for DBT it reached 78% (figure 8).

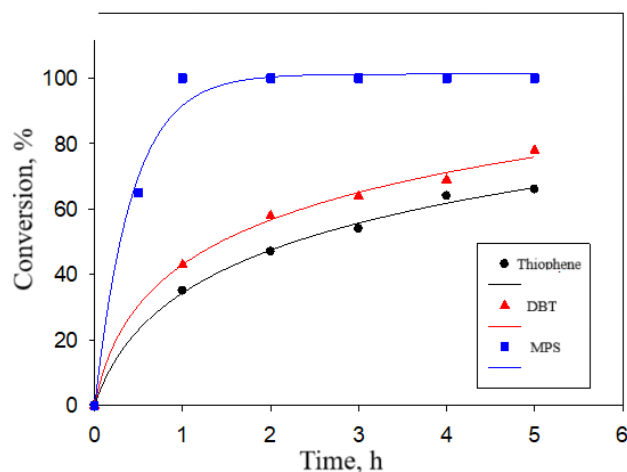


**Figure 6.** Conversion of model substrates as a function of time for the PMo–silica gel catalyst. Reaction conditions:  $V_{\text{solution}} = 10 \text{ ml}$ ,  $m_{\text{kat}} = 0,08 \text{ g}$ ,  $V_{\text{H}_2\text{O}_2} = 0,8 \text{ ml}$ ,  $T = 60^\circ\text{C}$ ,  $t = 5 \text{ h}$

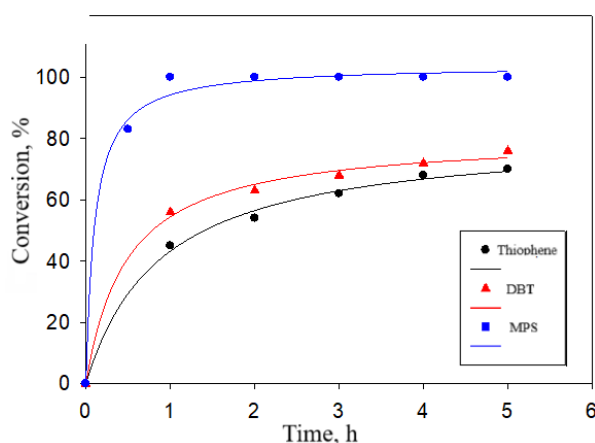


**Figure 7.** Conversion of model substrates as a function of time for the PW–silica gel catalyst. Reaction conditions:  $V_{\text{solution}} = 10 \text{ ml}$ ,  $m_{\text{kat}} = 0,08 \text{ g}$ ,  $V_{\text{H}_2\text{O}_2} = 0,8 \text{ ml}$ ,  $T = 60^\circ\text{C}$ ,  $t = 5 \text{ h}$

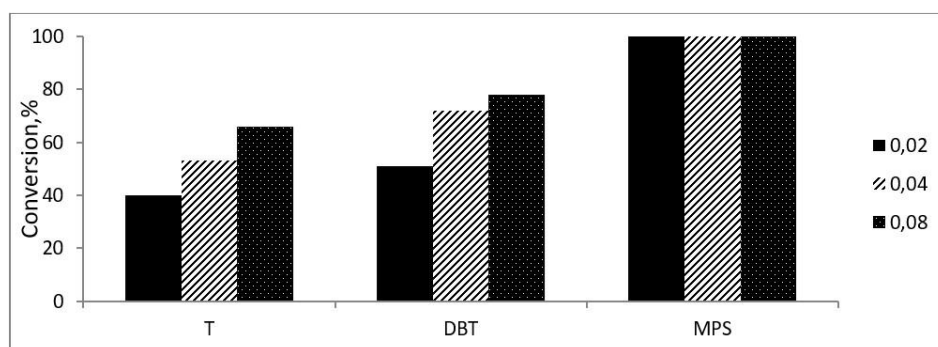


**Figure 8.** Effect of catalyst loading of PMo–silica gel on the conversion of model substrates  
Reaction conditions:  $V_{\text{solution}} = 10 \text{ ml}$ ,  $m_{\text{cat}} = 0.02 - 0.08 \text{ g}$ ,  $V_{\text{H}_2\text{O}_2} = 0.8 \text{ ml}$ ,  $T = 60^\circ\text{C}$ ,  $t = 5 \text{ h}$

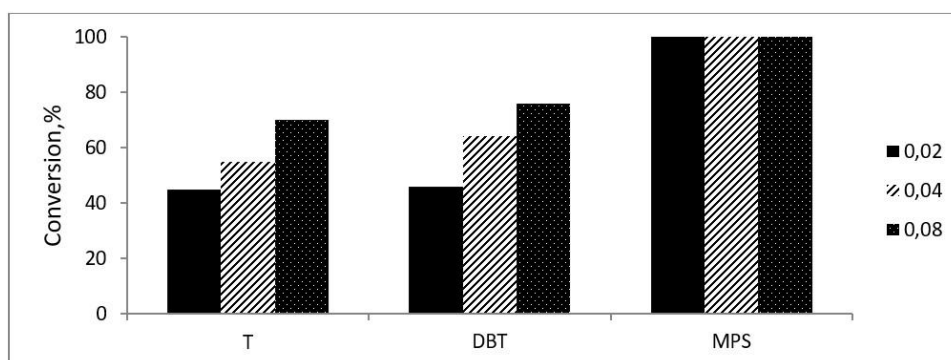


**Figure 9.** Effect of catalyst loading of PW–silica gel on the conversion of model substrates  
Reaction conditions:  $V_{\text{solution}} = 10 \text{ ml}$ ,  $m_{\text{cat}} = 0.02 - 0.08 \text{ g}$ ,  $V_{\text{H}_2\text{O}_2} = 0.8 \text{ ml}$ ,  $T = 60^\circ\text{C}$ ,  $t = 5 \text{ h}$

For the PW–silica gel catalyst (figure 9), the conversion of thiophene was higher than that observed for the PMo–silica gel catalyst, reaching 70%. In contrast, in DBT oxidation this catalyst proved to be less active, with a conversion of 76%. It is worth noting that this trend was also characteristic of the Silochrom-supported systems, where the W-containing catalyst exhibited higher activity in thiophene oxidation, while the Mo-containing catalyst was more efficient in DBT oxidation. Both systems were also active in the oxidation of MFSCs, achieving 100% conversion [26–28].

Variation in the amount of hydrogen peroxide had a significant effect on the conversion of both thiophene and DBT for the PMo–silica gel catalyst across the entire concentration range. The best results in the oxidation of thiophene and DBT were obtained at an excess of  $\text{H}_2\text{O}_2$ :S = 20:1 (figure 10).

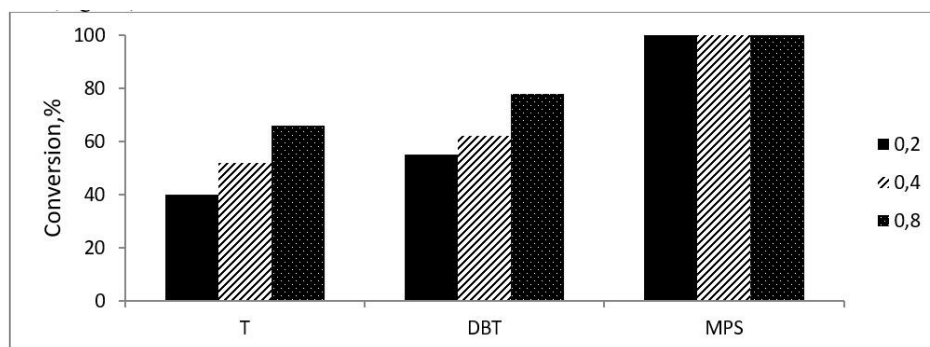


**Figure 10.** Effect of  $\text{H}_2\text{O}_2$  volume (mL) on the conversion of model substrates over the PMo–silica gel catalyst

Reaction conditions:  $V_{\text{solution}} = 10 \text{ ml}$ ,  $m_{\text{cat}} = 0.08 \text{ g}$ ,  $V_{\text{H}_2\text{O}_2} = 0.2 - 0.8 \text{ ml}$ ,  $T = 60^\circ\text{C}$ ,  $t = 5 \text{ h}$

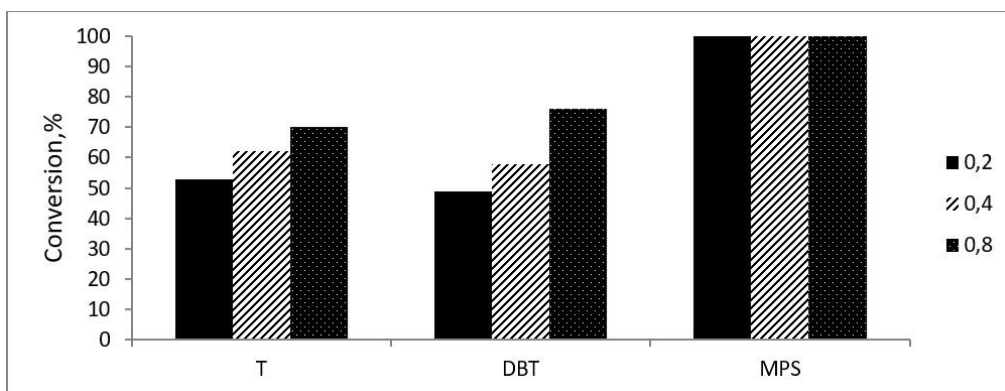


**Figure 11.** Effect of H<sub>2</sub>O<sub>2</sub> volume (mL) on the conversion of model substrates over the PW–silica gel catalyst

Reaction conditions:  $V_{solution} = 10\text{ ml}$ ,  $m_{kat} = 0,08\text{ g}$ ,  $V_{H2O2} = 0,2 - 0,8\text{ ml}$ ,  $T = 60^{\circ}\text{C}$ ,  $t = 5\text{ h}$

The dependence of thiophene and DBT conversion on the oxidant volume for the PW–silica gel catalyst was similar (figure 11). For both systems, oxidation of MFSCs proceeded with maximum conversion even at low oxidant volumes.

With sequential addition of the oxidant (figure 12), the conversion of thiophene was increased, reaching a maximum of 72%.

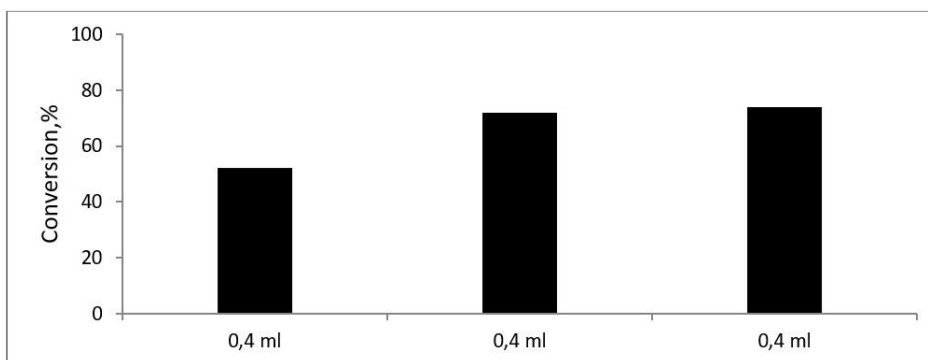


**Figure 12.** Sequential addition of H<sub>2</sub>O<sub>2</sub> using the PMo–silica gel catalyst as an example.

Reaction conditions:  $V_{solution} = 10\text{ ml}$ ,  $m_{kat} = 0,08\text{ g}$ ,  $T = 60^{\circ}\text{C}$ ,  $t = 5\text{ h}$

While the conversion of MFSCs (figure 13) did not change and remained at the maximum level over five consecutive oxidation cycles.

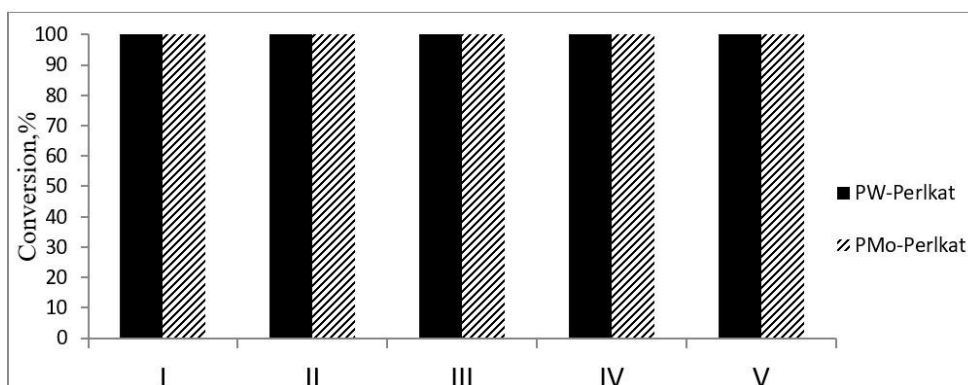


**Figure 13.** Conversion of MFSCs over five consecutive cycles on PMo–silica gel and PW–silica gel catalysts.

Reaction conditions:  $0.02\text{ g catalyst} + 0.8\text{ ml H}_2\text{O}_2$  at  $60^{\circ}\text{C}$ ,  $3\text{ h}$ .

At the same time, it should be noted that the silica gel-supported catalysts exhibit smaller fluctuations in conversion values from cycle to cycle, which overall characterizes them as more stable compared to the Silochrom-supported samples.

#### 4. Conclusion

This study demonstrates that PMo and PW heteropoly acids immobilized on silica gel are efficient and recyclable catalysts for oxidative desulfurization under mild conditions. The Mo-containing system exhibited higher activity toward DBT, while the W-containing catalyst was more effective for thiophene oxidation. Both systems achieved complete conversion of model fuel sulfur compounds and maintained stable performance over five consecutive cycles, outperforming Silochrom-supported analogues in terms of recyclability. Overall, the results highlight silica gel as a promising support for polyoxometalate-based catalysts for the production of ultra-low sulfur fuels.

#### Acknowledgment

The present study was conducted as part of the ongoing scientific cooperation between the Azerbaijan State Oil and Industry University, the A.N. Frumkin Institute of Physical Chemistry and Electrochemistry (RAS), and the Department of Chemistry of Moscow State University. The authors gratefully acknowledge the support and collaboration provided by these institutions.

#### Authors' Declaration

The authors declare that the work presented in this manuscript is original and has not been published or submitted elsewhere in any form. All authors have read and approved the final version of the manuscript and agree with its submission to the journal. The authors also confirm that there are no conflicts of interest related to this study.

#### Authors' Contribution Statement

All authors contributed equally to the conception, experimental design, data collection, and analysis of the study. They jointly participated in both the theoretical investigation and experimental validation of the results. The manuscript was written and revised through mutual collaboration, and all authors approved the final version of the paper.

#### References

1. K. Stawicka, J. Gajewska, M. Ziolk, M. Trejda, *Molecules* **30**(3) (2025) 551.
2. Q. Wang, T. Huang, S. Tong, C. Wang, H. Li, M. Zhang, *Molecules* **29**(7) (2024) 1548.
3. P.D. Polikarpova, A.O. Koptelova, A.V. Vutolkina, A.V. Akopyan, *ACS Omega* **7**(51) (2022) 48349.
4. S.W. Lee, P.D.Q. Dao, H.-J. Lim, C.S. Cho, *ACS Omega* **7**(22) (2022) 18486.
5. S.J.C. Ng, A.E.S. Choi, *Results in Engineering* **21** (2025) 106577.
6. K.M. Sarkarabad, A. Ghaemi, *Case Studies in Chemical and Environmental Engineering* **12** (2025) 101164.
7. N.V. Maksimchuk, O.A. Kholdeeva, *Catalysts* **13**(2) (2023) 360.
8. B. Yuan, X. Li, Y. Sun, *Catalysts* **12**(2) (2022) 129.
9. S. Tong, T. Huang, M. Chen, Z. Zhu, C. Wang, H. Li, M. Zhang, *Catalysts* **14**(11) (2024) 796.
10. S.O. Ribeiro, C. Granadeiro, M.C. Corvo, J. Pires, J.M. Campos-Martin, B. de Castro, S.S. Balula, *Frontiers in Chemistry* **7** (2019) 756.
11. H. Miao, M. Li, F. Wang, J. Li, Y.W. Lin, J. Xu, *Frontiers in Bioengineering and Biotechnology* **10** (2022) 907855.
12. B. Wang, B. Dai, M. Zhu, *ACS Omega* **5**(1) (2020) 378.

13. W.H. Müller, A. Verdin, E. De Pauw, C. Malherbe, G. Eppe, *Mass Spectrometry Reviews* **41**(3) (2022) 373.
14. J.E. Boulicault, S. Alves, R.B. Cole, *J. Am. Soc. Mass Spectrom.* **27**(8) (2016) 1301.
15. C.N. Dias, I.C.M.S. Santos-Vieira, C.R. Gomes, F. Mirante, S.S. Balula, *Nanomaterials* **14**(9) (2024) 733.
16. J. Ortiz-Bustos, et al., *Dalton Transactions* **52**(34) (2023) 12475.
17. J. Zhang, L. Sun, H. Chen, W. Zhao, C. Liu, et al., *Applied Organometallic Chemistry* **38**(3) (2024) e7610.
18. J. Li, J. He, Md.T. Aziz, X. Song, Y. Zhang, Z. Niu, *Journal of Hazardous Materials* **414** (2021) 125461.
19. A.K. Buryak, *Mass Spectrometry Reviews* **31**(2) (2012) 86.
20. M.N. Hossain, H.C. Park, H.S. Choi, *Catalysts* **9**(3) (2019) 229.
21. B. Barghi, A. Malekzadeh, M. Khosravi, *ACS Omega* **7** (2022) 12537.
22. J.M. Conesa, et al., *Catalysis Today* **418** (2023) 86.
23. S.S. Mgiba, V. Mhuka, N.C. Hintsho-Mbita, N. Mketi, *Chemical Papers* **78** (2024) 5275.
24. M. Bandyopadhyay, D. Jadav, N. Tsunoji, T. Sano, M. Sadakane, *Reaction Kinetics, Mechanisms and Catalysis* **128**(1) (2019) 139.
25. A. Wesner, N. Herrmann, L. Prawitt, A. Ortmann, J. Albert, M.J. Poller, *RSC Advances* **1** (2025) 10234.
26. E. Rafiee, F. Darvishi, *Petroleum Science and Technology* **34** (2016) 1201.
27. F. Ferella, et al., *Journal of Molecular Catalysis A: Chemical* **499** (2020) 111263.
28. T. Pei, et al., *Catalysts* **13** (2023) 631.